Research Square

Preprints are preliminary reports that have not undergone peer review.
They should not be considered conclusive, used to inform clinical practice,
or referenced by the media as validated information.

Structural, Dielectric and Thermal Properties of PVDF - Nickel Metal Organic Framework (Ni-MOF) Nanocomposites

Vikas Rathour
PDPM- Indian Institute of Information Technology, Design and Manufacturing
R. K. Tiwari
Hindustan College of Science and Technology
Sergej Iľkovič
University of Prešov
Rohan Sagar
Hindustan College of Science and Technology
Pramod Kumar Singh
Hindustan College of Science and Technology
M. S. Gaur
ms.gaur.hcst@sgei.org
Hindustan College of Science and Technology
M. K. Roy
PDPM- Indian Institute of Information Technology, Design and Manufacturing

Research Article

Keywords: SEM, XRD, Dielectric permittivity, DSC, TGA

Posted Date: March 23rd, 2026

DOI: https://doi.org/10.21203/rs.3.rs-8782231/v1

License: This work is licensed under a Creative Commons Attribution 4.0 International License.
Read Full License

Additional Declarations: No competing interests reported.

Structural, Dielectric and Thermal Properties of PVDF - Nickel Metal Organic Framework (Ni-MOF) Nanocomposites

Vikas Rathour[1], R. K. Tiwari[2], Sergej Ilʹkovič[3], Rohan Sagar[2], Pramod Kumar Singh[2], M. S. Gaur[2*], M. K. Roy[1]

[1]*Department of Natural Science, PDPM- Indian Institute of Information Technology, Design and Manufacturing, Jabalpur, Madhya Pradesh, 482005, India*
[2]*Department of Physics, Hindustan College of Science and Technology, Farah, Mathura, U.P. 281122, India*
[3]*Faculty of Humanities and Natural Sciences, Presov University, Presov, Republic of Slovakia*

*****Corresponding author: ms.gaur.hcst@sgei.org

Abstract

In this work, we introduce a metal-organic framework (MOF) that is 2D in nature into the poly (vinylidene fluoride) (PVDF) matrix, an area relatively underexplored. Using the chemical method, a highly 2D Ni-MOF was synthesized. Ni-MOF with different weight ratios was incorporated into PVDF matrixes by solvent casting. SEM and XRD were used to determine the nanocomposite structure. According to XRD, PVDF shifted towards the β phase with the incorporation of Ni MOF nanofiller. **The dielectric constant decreases with frequency; however, higher MOF loadings cause the dielectric constant to decrease as dielectric loss increases.** TGA/DSC shows that the thermal stability of PVDF-Ni-MOF nanocomposite is higher than that of pure PVDF due to the intermolecular interaction of Ni-MOF with PVDF.

Keywords: SEM·XRD· Dielectric permittivity · DSC·TGA

Introduction

A typical ferroelectric polymer is poly (vinylidene fluoride), whose dielectric constant is 10. It also has a dielectric strength of 800 kV/mm. PVDF is an excellent chemical resistance ferroelectric polymer. The vinylidene fluoride in PVDF provides excellent corrosion and abrasion resistance, as well as excellent electro-active properties. **Recently, the addition of nanofillers has become a widely employed method for increasing the β-phase content in PVDF due to its simplicity and adaptability.** Adding nanofillers to PVDF to raise the β-phase content has become a common method lately because it is easy to use and can be changed to fit different needs. It is obvious that MOFs are very different from flexible polymers, thus scientists are trying to combine the two materials to make composites with the best qualities of each. To make MOFs, organic linkers are

linked to metal-inclusive units (MIUs) or secondary building units (SBUs). This creates open frameworks that are stable and have permanent porosity [1]. Nickel-based Metal-Organic Framework (Ni-MOF) facilitates the structural modification of Polyvinylidene Fluoride (PVDF) by promoting the development of the polar β-phase, thereby enhancing the material's piezoelectric characteristics. **This effect is realized through the integration of Ni-MOF into the PVDF matrix, which contributes to superior dielectric and energy storage capabilities** [2,3]. PVDF's electroactive properties are highly dependent on its polarity. **As a result, the α phase's TG^+ TG^- chain conformation changes to the TTTT and/or $T_3G^+T_3G^-$ chain conformations of the β and γ phases, respectively.** This is because the dipole alignment generated by this interaction [6,7]. Dielectric permittivity and piezoelectric activity of PVDF-based composite films are strongly affected by their amount of deuterium (exhibiting the highest dipole moment). A variety of unique techniques have been used to improve PVDF's polarity [4]. Among the various techniques investigated, nanomaterials have been incorporated directly into PVDF matrixes, a method that is both easy and cost-effective [4,5]. A fundamental goal of incorporating nanomaterials into PVDF is to induce strong interfacial interactions between PVDF dipoles ($–CH_2$ and $–CF_2$ dipoles) and their surfaces. Consequently, the TG^+ TG^-chain conformation of the α phase transforms to the TTTT and/or $T3G^+T3G^-$ chain conformations of the β and γ phases, respectively, through the dipole alignment caused by this interaction [6,7]. As electronics and electrical fields have grown rapidly in recent years, many electronic components have improved for greater intelligence, miniaturization, and integration, posing challenges to existing materials [8–12]. In order to fabricate promising flexible films with excellent electrical and mechanical properties on a large scale, it is necessary to find a concise and effective process. As opposed to traditional inorganic ceramics, flexible ferroelectric polymers have many advantages, including good toughness, ease of processing, and ease of integration [13–16]. In the present work, we prepare Ni-MOF and PVDF/Ni-MOF nanocomposite thin films and study their structural, thermal, and dielectric properties by SEM, XRD, TGA/DSC, and dielectric parameter (i.e., permittivity, dielectric loss, AC conductivity, and impedance) measurements and develop correlations with these properties.

Experimental Techniques

The granular PVDF used in this investigation was purchased from Redox (India), while Merck provided the methanol, N, and N-Dimethylformamide (DMF). For MOF synthesis, $NiCl_2.6H_2O$ (98%; Merk) was used as a source of metal ions, and trimesic acid (TMA, 99%; Merck) was used

as an organic linker. To modify the pH, sodium hydroxide (99%; Sigma Aldrich) DI water (18.3 MΩ cm) was used. We employed laboratory-grade reagents and solvents in the synthesis without any further steps to clean them up. We can make MOFs using Ni (II) metal ions using aqueous solutions of Ni (II) metal ions, which is a method that has already been reported. To prepare an aqueous solution, 50 mL of deionized (DI) water was added with 4.75×10^{-3} mol of trimesic acid (TMA). We added drops of a 1 M NaOH solution to the organic linker solutions until the pH reached 7, and 50-mL DI water was used to prepare metal ion solutions containing 3.72×10^{-3} mol of Ni (II). The prepared metal ion solutions were introduced dropwise into the TMA, solution in a beaker while being continuously stirred at a rate of 1000 rpm using a separator beaker. The light green precipitate was seen upon completion with TMA and mixing proceeded for 12 hours. Finally, the MOFs were filtered through filter paper, rinsed twice with ethanol and extra water, and then dried for five hours at 70 °C and then for another 48 hours at 100 °C. The TMA-M Ni (II) MOFs that were made were stored in sealed containers so they could be used later in experiments [17,18]. **DSC (Differential Scanning Calorimetry) measurements are typically conducted to ensure accurate and reproducible results in a nitrogen atmosphere with a heating rate of 10^0C/ min using DSC Q200. The instrument was calibrated using standard materials to ensure accurate temperature and heat flow measurements. The 5 mg sample was taken and placed in a suitable pan for analysis. A common method for frequency-dependent dielectric measurement involves using a precision LCR meter model no. Novacontrol Technology. The Al coated circular sample of diameter 1 cm is placed between electrodes, and the device applies an AC voltage at varying frequencies. The resulting capacitance was measured to calculate dielectric constant and loss tangent, as a function of frequency.**

Preparation of PVDF-Ni-MOF nanocomposites

Solution casting was used to mix MOF with PVDF to form nanocomposite thin films. By dissolving 5gm of PVDF in 100 ml of N-dimethylformamide (DMF), the PVDF-Ni MOF nanocomposite was produced, which was then magnetically stirred at 60°C for 6 hours. To create PVDF-Ni MOF nanocomposite samples, Dimethylformamide (DMF) with Ni MOF (0.20 g for 4%) was dissolved. A magnetic stirrer was used to agitate these solutions for 12 hours to attain homogeneity. After the solution had been prepared, it was placed in a sonicator set at 20 kHz for 10 minutes to disperse Ni MOF in PVDF solution[19]. A glass plate was poured with the prepared

solution. The solvent was allowed to evaporate in a room temperature oven for a whole day, producing nanocomposite films. The thin nanocomposite films were very easy to remove from the glass plates. After drying, the films were vacuumed to 10^{-5} Torr for 48 hours at 30^0C to remove any leftover solvent. To measure the thickness of the film, an electronic screw gauge was employed. For the SEM, XRD, and dielectric analysis, the samples had a thickness of 30–50μm.

Results and Discussion

Scanning Electron Microscopy (SEM)

Fig. 1(a) shows an SEM picture of the produced Ni-MOF particles with a magnification of 5.0 KX. The particles are small, but the micrograph shows that there are larger secondary aggregates that formed when particles interacted with each other. This renders it to appear like the particles are bigger than they genuinely are. At a low concentration of Ni-MOF (4 wt%), the PVDF matrix shows a spherulitic microstructure that is comparable to that of pure PVDF with α- and β-phases, as seen in Fig. 1(b) [20]. At this loading, the nanofiller primarily influences the nucleation process, and the overall spherulitic structure of PVDF remains mostly unchanged. As the amount of Ni-MOF increases (8 and 12 wt.%), the spherulitic structure of PVDF becomes increasingly disintegrated, as shown in Fig. 1(c) and Fig. 1(d). At these higher filler concentrations, the Ni-MOF particles accumulate together in large clusters that are not uniformly distributed throughout the polymer matrix. This kind of agglomeration slows down the growth of spherulites and changes the rate of crystallization, which changes the polymer phase and lowers the degree of crystallinity [21]. In these composites, the polymer phase is limited to smaller regions between MOF aggregates, which stops crystals from growing. Thereby, the most effective way to disperse Ni-MOF in the PVDF matrix is at low filler concentrations. At larger concentrations, the particles adhere together, and the microstructure becomes uneven.

X-ray diffraction (XRD)

Fig. 2 displays the XRD patterns of pristine PVDF and PVDF–Ni-MOF nanocomposite thin films with Ni-MOF loadings of 4, 8, and 12 wt%. The XRD pattern of pure PVDF shows a strong diffraction peak at $2\theta = 19.25°$, which is the (110)/ (200) planes of the polar β-phase. When 4 wt% Ni-MOF is added, new diffraction peaks show up at $2\theta \approx 18.26°$ and 19.22°. These peaks are linked to the (020) plane of the α-phase and the overlapping contributions from PVDF crystalline phases. This shows that when there is a small amount of Ni-MOF, it changes the way the PVDF

chains are arranged in crystals, which causes distinct phases to partially coexist. As the amount of Ni-MOF increases (8 and 12 wt%), the major diffraction peak shifts from $2\theta \approx 19.25°$ to $\approx 19.22°$, while the peak at 18.26° gets less intense. This behavior indicates a relative suppression of the non-polar α-phase and a stability of the polar β-phase at elevated filler concentrations, attributable to intensified interfacial contacts between Ni-MOF and PVDF dipoles. The β-phase content changes in a non-monotonic way because of the competing impacts of chain disruption caused by fillers at low loading and dipole alignment at moderate loading. In general, the overall degree of crystallinity goes down when the Ni-MOF content goes up (Table 1). This is something that is often seen in polymer nanocomposites. This decrease is due to the filler making it harder for polymer chains to move about and breaking up long-range crystalline order. When polymer chains stick to the filler surface, they become less available for crystallization [22]. The comparatively greater peak intensities seen in 8 and 12 wt% Ni-MOF composites suggest that the crystallites are oriented in a certain way, not that the overall crystallinity has gone up. Kinematical scattering theory posits that peak broadening in XRD patterns correlates with diminished crystallite size and heightened lattice disorder, both of which align with filler-induced confinement effects in PVDF-based nanocomposites [23–25].

Dielectric Properties

The dielectric response as a function of frequency was measured for the PVDF-Ni-MOF nanocomposites. Fig. 3 shows how the dielectric properties of PVDF films changed with increasing MOF content in the composites. Fig.3 and Fig.4 reveals that both the real part of the dielectric constant and the dielectric losses show similar behavior as the pure polymer, such as decrease with frequency. The relaxation process is assigned to cooperative segmental motions within the amorphous phase, which are also present in the nanocomposites [26]. Space charge increases in low-frequency regions because charge carriers have more time to accumulate under the electric field, leading to higher density. Space charge accumulation generally increases the dielectric constant by enhancing polarization, especially at low frequencies. However, at higher frequencies or under specific conditions, it can reduce the dielectric constant due to charge trapping and diminished polarization [27]**.** The MOF aggregates or touching particles have a significant impact on the effective dielectric permittivity and increase the local field in PVDF's ferroelectric phase. It is important to consider the specific microstructure when determining the field distribution and effective dielectric constant. The ferroelectric phase of PVDF is surrounded by

MOF with a low dielectric constant and a thin shell. On the shell, there is a high concentration of the local field, and on the ferroelectric phase, the field is almost zero, and on the matrix, it is nearly the same as that applied to the matrix. As the dielectric permittivity of the shell material increases, the electric field in the matrix becomes less homogeneous [28]. The explanation of local electric fields in a PVDF comprising a shell, ferroelectric phase, and matrix can be derived from the distinct dielectric properties of these components (i.e., in present case PVDF and Ni-MOF) and their interactions with an external electric field. The shell, characterized by a high permittivity, concentrates electric field lines within itself, resulting in a pronounced local field. In the ferroelectric phase, the material's inherent spontaneous polarization effectively mitigates the external field, leading to a near-zero field. Conversely, the matrix, with its lower permittivity, exhibits a field that closely resembles the applied field [29]. All composites have a decrease in dielectric constant as the frequency increases. This phenomenon can be explained by the relaxation of polarization at interfaces and dipole orientations within composites. **The PVDF composite with 4 wt% Ni-MOF has the highest dielectric constant of all the compositions because it has more dipolar and interfacial polarization. At higher filler loadings, though, Ni-MOF agglomeration renders it difficult for dipoles to migrate, which lowers the effective polarization and dielectric constant.** The polarizability may decrease when nanofillers agglomerate together, even with an electric field present [30]. This happens particularly in case of PVDF with 8% and 12% Ni-MOF. The substantial reduction in the dielectric constant value is attributed to a decrease in polarized dipoles within the nanocomposite, which is associated with the presence of the low β -crystal structure, as confirmed by XRD analysis. The decrease in real part of dielectric permittivity with increasing nanofiller concentration can occur due to factors such as agglomeration, increased dielectric loss, or a shift in the dominant polarization mechanisms at higher filler loadings. For example, in a study on barium titanate ($BaTiO_3$) nanofillers in a polymer matrix, the dielectric permittivity initially increased up to a certain concentration but began to decline as agglomeration became more pronounced at higher loadings. Similarly, in composites with silica nanoparticles, a significant increase in dielectric loss was observed at higher concentrations, leading to a reduction in the overall permittivity [31]. The relations between the real part of the impedance (M′) with different frequencies are shown in Fig. 5. For all nanocomposites, the value of the real part (M′) varies with the increase in the Ni-MOF content inside the PVDF matrices [32–34]**.** Increasing the Ni-MOF content in the PVDF results in a reduction in the real component of the electric modulus (M'). This indicates potential alterations

in the dielectric properties, which may be attributed to variations in polarization or charge carrier dynamics [35]. In the lower frequency range, M' exhibits an increasing trend with rising frequency. This phenomenon is attributed to the release of space charge, defined as the accumulation of charge carriers (electrons or ions) at interfaces or within the material under the influence of an applied electric field. This accumulation is particularly significant at lower frequencies, as the charge carriers are afforded more time to move and redistribute [36]. Dipoles in materials with higher inertia are unable to keep pace with field alternation. This phenomenon occurs because certain molecules or ions within the material exhibit greater resistance to altering their orientation in response to the electric field. At elevated frequencies these entities are unable to rotate or reposition swiftly, leading to a reduction in their contribution to polarization [37]**.** Fig.6 shows the plots between the imaginary part (M″) and the frequency. The M″ values decrease, and then become constant. The value of M″ is saturated toward higher frequency. This is an indication of the frequency dependency of the relaxation time in PVDF-Ni-MOF nanocomposites samples. The relaxation is due to the presence of inter-polarization (Maxwell–Wagner–Sillars polarization), which can usually be encountered inside the pure polymeric samples. This relaxation process is affected by the effect of the inter-polarization that causes the accumulation of electric charges around the molecules of the nanocomposite samples. As shown in Fig. 7, PVDF / PVDF-Ni-MOF nanocomposites exhibit AC conductivity between 10 Hz and 10^6 Hz at room temperature. Increasing frequency leads to a continuous increase in AC conductivity as shown in Fig.7. For PVDF-4% Ni MOF nanocomposites, AC conductivity, is the maximum. The increase in applied field frequency may have resulted in increased electron mobility, resulting in higher conductivity [38]. Additionally, at higher frequencies, the loss factor dominates, resulting in higher conductivity. As a consequence of the AC conductivity study, we can conclude that the relaxation mechanism is strongly dependent on composition.

Thermal properties

Thermogravimetric analysis (TGA)

We have investigated PVDF thermal stability with different concentrations of Ni-MOF nanofiller by using TGA analysis. As can be seen in Fig.8, all the samples examined degraded in a single step at 600°C almost without residual weight. Ni-MOF nanofiller increase the thermal stability of nanocomposites by shifting the onset decomposition temperatures higher side. A strong interfacial

interaction between PVDF and Ni-MOF contributes to the higher temperature shifting [39,40]. A variation in temperature was observed at every filler loading concentration at the end of thermal degradation (T_p). The highest results were observed at load concentrations of 12 wt%. Compared to PVDF, PVDF-Ni-MOF nanocomposites have a higher T_p at filler loadings of 4 and 8 wt%. This can be explained by a complex interfacial interaction between filler and matrix. This could be understood by interlocking carbon groups of polymers and nanofillers and the zigzag asperities in the molecular chains [41,42]. **Interlocking carbon groups in polymers and nanofillers refer to the structural arrangement where carbon atoms or groups in the molecular chains of polymers interact with nanofillers, creating a strong physical or chemical bond. These interactions enhance the mechanical and thermal properties of the composite material. Zigzag asperities in molecular chains describe the irregular, jagged features along the chain's structure, which can influence the interaction and alignment with nanofillers, contributing to improved load transfer and overall composite performance.**

Differential Scanning Calorimetry (DSC)

DSC can be used to distinguish PVDF phases, but it is not very reliable because of other factors, such as sample morphology, lamellar thickness, and crystal imperfection, can affect melting behavior as well. A melting peak on a DSC thermogram may also be a result of melting/recrystallizing during heating [43,44]. Fig. 9 shows the DSC thermograms of PVDF nanocomposites with compositional ratios wt.% of 4, 8, and 12% Ni-MOF. Each PVDF nanocomposite exhibits an endothermic peak between 140-150^{0}C. This peak is located near the melting temperature of pristine PVDF [45]**.** These DSC results are identical to other PVDF nanocomposite samples. There is a single peak associated with the PVDF structure, indicating polymorphic crystallization (i.e., higher temperature attributable to the β-phase) [46,47]. The lower temperature peak is reported to be due to the α-phase of PVDF. These results indicate the α phase of PVDF is not observed by DSC. The lowering of peak temperature values of PVDF-Ni-MOF nanocomposite is the evidence for the formation of PVDF heterogeneous chain interactions[48]. It was observed that in the presence of Ni-MOF, the functional groups of PVDF chains participated primarily in dipolar interactions and modified the polymer crystals' thermal behavior. Recent publications [49,50] demonstrate in detail the significance of a single peak related to an endothermic peak. According to the estimated degree of crystallinity, it ranged between 42% and 47%. It was noted that the degree of crystallinity decreased as Ni- MOF content increased (i.e.

Table 2). This behavior could be due to the possible changes in the quality of the PVDF / Ni-MOF dispersions during sample formation caused by nanoparticle agglomeration. According to XRD analysis and literature data on PVDF nanocomposites (this needs to be verified), the obtained X_c values are consistent [51–53]. Namely, the crystallites of the β-phase are smaller than those of the α-phase, thus reducing the crystallinity in β-phase rich samples [54]. This behavior fully corresponds to β-phase PVDF.

Conclusions

As a result, PVDF-Ni MOF nanocomposites have been successfully prepared by the solution mixing method. It was investigated that, through structural studies, Ni-MOF influences PVDF dielectric and thermal properties. All testing indicated that MOF increased PVDF nanocomposite crystal content, resulting in a higher dielectric permittivity, lower dielectric loss, increased residual polarization, and an increase in the need for electric applications with the PVDF nanocomposite. X-ray diffraction (XRD) analysis of the nanocomposites confirms the formation of the β phase of PVDF upon the addition of Ni-MOF. Due to the presence of Ni-MOF, there is a possibility of structural reorganization in the polymer chain. This leads to a decrease in polymer crystallinity. The DSC study further confirms the presence of a strong β phase. As the thermal degradation test from the TGA/DSC instrument indicates, there is only one stage during the decomposition process for all PVD / Ni-MOF nanocomposites. However, PVDF-Ni-MOF nanocomposite thermal properties are higher than those of pure PVDF. **The combined structural, dielectric, and thermal properties indicate that PVDF–Ni-MOF nanocomposites are viable candidates for applications necessitating flexible dielectric materials with improved thermal stability. Future research may concentrate on enhancing filler dispersion, regulating interfacial interactions, and customizing MOF chemistry to further elevate dielectric performance, energy storage capacity, and multifunctional characteristics for application in sensors, capacitors, and polymer-based electronic devices.**

Acknowledgments

Vikas Rathour, is immensely thankful to the Ministry of Education (MoE), Government of India for providing a doctoral fellowship. Prof. M. S. Gaur is thankful to Slovakia Government for awarding National Slovak Scholarship for international university teachers, researchers and artist.

Authors Contribution

Vikas Rathour: Conceptualization, Writing, Data curation, Synthesis and Characterization, R. K. Tiwari: Editing, Review, Sergej Iľkovič: Editing, Review, Rohan Sagar: Editing, Review, Pramod Kumar Singh: Editing, Review, M.K.Roy: Review, supervision, M.S.Gaur: Review, Editing and Supervision

Declarations

Conflict of interest: The authors declare no conflicts of interest.

References

1. Deeraj BDS, Jayan JS, Raman A, Asok A, Paul R, Saritha A, et al. A comprehensive review of recent developments in metal-organic framework/polymer composites and their applications. Surfaces and Interfaces. 2023;43:103574.

2. Kalaj M, Bentz KC, Ayala SJr, Palomba JM, Barcus KS, Katayama Y, et al. MOF-Polymer Hybrid Materials: From Simple Composites to Tailored Architectures. Chem Rev. 2020;120:8267–302.

3. Gui Y, He S, Wang Y, Yang J. MOF-derived porous Ni/C material for high-performance hybrid nanogenerator and self-powered wearable sensor. Composites Part A: Applied Science and Manufacturing. 2023;168:107492.

4. Padurariu L, Horchidan N, Ciomaga CE, Curecheriu LP, Lukacs VA, Stirbu RS, et al. Influence of Ferroelectric Filler Size and Clustering on the Electrical Properties of (Ag–BaTiO3)–PVDF Sub-Percolative Hybrid Composites. ACS Appl Mater Interfaces. 2023;15:5744–59.

5. Sasmal A, Patra A, Devi PS, Sen S. Hydroxylated $BiFeO_3$ as efficient fillers in poly(vinylidene fluoride) for flexible dielectric, ferroelectric, energy storage and mechanical energy harvesting application. Dalton Trans. 2021;50:1824–37.

6. Agayev FG, Trukhanov SV, Trukhanov AnV, Jabarov SH, Ayyubova GSh, Mirzayev MN, et al. Study of structural features and thermal properties of barium hexaferrite upon indium doping. J Therm Anal Calorim. 2022;147:14107–14.

7. Jiang J, Li J, Zhang Y, Yuan Y, Liu X, Zuo P, et al. Tuning the interfacial insulating shell characteristics in $CaCu_3Ti_4O_{12}$ nanowires/polyetherimide nanocomposites for high-temperature capacitive energy storage. J Mater Chem C. 2022;10:7962–9.

8. Li Z, Stoffel M, Ding L, Rouxel D, Ding Q. Synthesis of hydrophilic P(VDF-TrFE) chloride sensitive polymer films for fluorescence sensing. J Polym Res. 2019;26:269.

9. Zhang Y, Zhang C, Feng Y, Zhang T, Chen Q, Chi Q, et al. Excellent energy storage performance and thermal property of polymer-based composite induced by multifunctional one-dimensional nanofibers oriented in-plane direction. Nano Energy. 2019;56:138–50.

10. Yan Z, Yang Y, Cai X. Preparation of a ferroelectric composite film metal–organic framework/PVDF. J Polym Res. 2020;27:377.

11. Zak AK, Gan WC, Majid WHAbd, Darroudi M, Velayutham TS. Experimental and theoretical dielectric studies of PVDF/PZT nanocomposite thin films. Ceramics International. 2011;37:1653–60.

12. Guo M, Jiang J, Shen Z, Lin Y, Nan C-W, Shen Y. High-Energy-Density Ferroelectric Polymer Nanocomposites for Capacitive Energy Storage: Enhanced Breakdown Strength and Improved Discharge Efficiency. Materials Today. 2019;29:49–67.

13. Navalón S, Dhakshinamoorthy A, Álvaro M, Ferrer B, García H. Metal–Organic Frameworks as Photocatalysts for Solar-Driven Overall Water Splitting. Chem Rev. 2023;123:445–90.

14. Feng Y, Zhou Y, Zhang T, Zhang C, Zhang Y, Zhang Y, et al. Ultrahigh discharge efficiency and excellent energy density in oriented core-shell nanofiber-polyetherimide composites. Energy Storage Materials. 2020;25:180–92.

15. Prateek, Thakur VK, Gupta RK. Recent Progress on Ferroelectric Polymer-Based Nanocomposites for High Energy Density Capacitors: Synthesis, Dielectric Properties, and Future Aspects. Chem Rev. 2016;116:4260–317.

16. Shimizu H, Li Y, Kaito A, Sano H. High-shear effects on the nano-dispersed structure of the PVDF/PA11 blends. J Nanosci Nanotechnol. 2006;6:3923–8.

17. Sahiner N, Sel K, Ozturk OF, Demirci S, Terzi G. Facile synthesis and characterization of trimesic acid-Cu based metal organic frameworks. Applied Surface Science. 2014;314:663–9.

18. Sel K, Demirci S, Meydan E, Yildiz S, Ozturk OF, Al-Lohedan H, et al. Benign Preparation of Metal–Organic Frameworks of Trimesic Acid and Cu, Co or Ni for Potential Sensor Applications. J Electron Mater. 2015;44:136–43.

19. Indolia AP, Gaur MS. Optical properties of solution grown PVDF-ZnO nanocomposite thin films. J Polym Res. 2013;20:43.

20. Ye Q, Xu J-M, Zhang Y-J, Chen S-H, Zhan X-Q, Ni W, et al. Metal-organic framework modified hydrophilic polyvinylidene fluoride porous membrane for efficient degerming selective oil/water emulsion separation. npj Clean Water. 2022;5:1–9.

21. Costa CM, Firmino Mendes S, Sencadas V, Ferreira A, Gregorio R, Gómez Ribelles JL, et al. Influence of processing parameters on the polymer phase, microstructure and macroscopic properties of poly(vinilidene fluoride)/Pb(Zr0.53Ti0.47)O_3 composites. Journal of Non-Crystalline Solids. 2010;356:2127–33.

22. Varkalis A, Gedde UW. Crystallinity of filled compositions of low-density polyethylene and poly(ethylene-co-vinyl acetate). Thermochimica Acta. 1993;214:123–8.

23. Fan H, Peng Y, Li Z, Chen P, Jiang Q, Wang S. Preparation and characterization of hydrophobic PVDF membranes by vapor-induced phase separation and application in vacuum membrane distillation. J Polym Res. 2013;20:134.

24. Shen Y, Hu Y, Chen W, Wang J, Guan Y, Du J, et al. Modulation of topological structure induces ultrahigh energy density of graphene/Ba0.6Sr0.4TiO3 nanofiber/polymer nanocomposites. Nano Energy. 2015;18:176–86.

25. Golcuk S, Muftuoglu AE, Celik SU, Bozkurt A. Synthesis and characterization of polymer electrolyte membranes based on PVDF and styrene via photoinduced grafting. J Polym Res. 2013;20:144.

26. Martins P, Costa CM, Botelho G, Lanceros-Mendez S, Barandiaran JM, Gutierrez J. Dielectric and magnetic properties of ferrite/poly(vinylidene fluoride) nanocomposites. Materials Chemistry and Physics. 2012;131:698–705.

27. Li G, Liu T, Gu Z, Chen X, Sun B, Zhu Y, et al. Space charge characteristics and dielectric properties of PANI/PP-g-MAH/PP ternary composite. High Voltage. 2025;10:178–85.

28. Padurariu L, Brunengo E, Canu G, Curecheriu LP, Conzatti L, Buscaglia MT, et al. Role of Microstructures in the Dielectric Properties of PVDF-Based Nanocomposites Containing High-Permittivity Fillers for Energy Storage. ACS Appl Mater Interfaces. 2023;15:13535–44.

29. Zhong S-L, Dang Z-M, Zhou W-Y, Cai H-W. Past and future on nanodielectrics. IET Nanodielectrics. 2018;1:41–7.

30. Jamail N a. M, Piah M a. M, Muhamad NA, Salam Z, Kasri NF, Zainir RA, et al. Effect of Nanofillers on the Polarization and Depolarization Current Characteristics of New LLDPE-NR Compound for High Voltage Application. Advances in Materials Science and Engineering. 2014;2014:416420.

31. Ye H, Chen H, Zhang X, Chen Y, Shao W, Xu L. Electron structure in modified BaTiO3 /poly(vinylidene fluoride) nanocomposite with high dielectric property and energy density. IET Nanodielectrics. 2019;2:70–7.

32. Hamzah M, Saion E, Kassim A, Hussain M, Shahrim I, Ali Omer M. Temperature Dependence of AC Electrical Conductivity of PVA-PPy-FeCl3 Composite Polymer Films. Malaysian Polym J. 2008;3.

33. Sengwa RJ, Dhatarwal P. Predominantly chain segmental relaxation dependent ionic conductivity of multiphase semicrystalline PVDF/PEO/LiClO4 solid polymer electrolytes. Electrochimica Acta. 2020;338:135890.

34. Puértolas JA, García-García JF, Pascual FJ, González-Domínguez JM, Martínez MT, Ansón-Casaos A. Dielectric behavior and electrical conductivity of PVDF filled with functionalized single-walled carbon nanotubes. Composites Science and Technology. 2017;152:263–74.

35. Duta L, Grumezescu V. The Effect of Doping on the Electrical and Dielectric Properties of Hydroxyapatite for Medical Applications: From Powders to Thin Films. Materials. 2024;17:640.

36. Gozzo CB, Terezo AJ, Thaines EHNS, Sales AJM, Freitas RG, Sombra ASB, et al. Effects of MgO on dielectric relaxation and phase transition of the ceramic matrix BaBi4Ti4O15. Journal of Science: Advanced Materials and Devices. 2019;4:170–9.

37. Kavinkumar T, Manivannan S. Thermal and dielectric properties of multi-walled carbon nanotube–graphene oxide composite. J Mater Sci: Mater Electron. 2017;28:344–53.

38. Ojha S, Ali MS, Roy M, Bhattacharya S. Hopping frequency and conductivity relaxation of promising chalcogenides: AC conductivity and dielectric relaxation approaches. Mater Res Express. 2021;8:085203.

39. Begum S, Ullah H, Ahmed I, Zhan Y, Kausar A, Aleem MA, et al. Investigation of morphology, crystallinity, thermal stability, piezoelectricity and conductivity of PVDF nanocomposites reinforced with epoxy functionalized MWCNTs. Composites Science and Technology. 2021;211:108841.

40. Li W, Li H, Zhang Y-M. Preparation and investigation of PVDF/PMMA/TiO2 composite film. J Mater Sci. 2009;44:2977–84.

41. Yadav V, Pal D, Poonia AK. Nanofillers as a potential key for shaping the future of the industries. Hybrid Advances. 2024;7:100340.

42. Yesaswi ChS, Satya SK, Sahu SK, Badgayan ND, Sri Ram Murthy P, Kumar VMR, et al. 6 - Thermal properties of polymer nanocomposites. In: Hoque ME, Ramar K, Sharif A, editors. Advanced Polymer Nanocomposites. Woodhead Publishing; 2022.

43. Teyssedre G, Bernes A, Lacabanne C. Influence of the crystalline phase on the molecular mobility of PVDF. Journal of Polymer Science Part B: Polymer Physics. 1993;31:2027–34.

44. Pramoda K, Mohamed A, Yee Phang I, Liu T. Crystal transformation and thermomechanical properties of poly(vinylidene fluoride)/clay nanocomposites. Polymer International. 2005;54:226–32.

45. Mokhtari F, Spinks GM, Sayyar S, Foroughi J. Dynamic Mechanical and Creep Behaviour of Meltspun PVDF Nanocomposite Fibers. Nanomaterials. 2021;11:2153.

46. Dhatarwal P, Sengwa RJ. Crystalline Phases Thermal Behaviour, Optical Energy Band Gap, and Broadband Radio Wave Frequency Dielectric Properties of PEO/PVDF Blend Films. Macromol Res. 2022;30:460–9.

47. Mohamadi M. Interpretation of thermal transitions and phase transformations in semi-crystalline PVDF/PEO/graphene nanocomposites characterized by modulated-temperature DSC. J Therm Anal Calorim. 2022;147:6701–12.

48. Gregorio R Jr, Cestari M. Effect of crystallization temperature on the crystalline phase content and morphology of poly(vinylidene fluoride). Journal of Polymer Science Part B: Polymer Physics. 1994;32:859–70.

49. Sengwa RJ, Dhatarwal P. Crystalline phases thermal behaviour and radio frequencies dielectric properties of PVDF/PEO/metal oxides hybrid polymer nanocomposite films. J Polym Res. 2022;29:186.

50. Sengwa RJ, Dhatarwal P. Thermally improved crystalline phase and intercalated PEO/OMMT nanocomposites for high to ultrahigh radio frequency range low-permittivity nanodielectrics. Journal of Applied Polymer Science. 2022;139:51599.

51. Sekkarapatti Ramasamy M, Rahaman A, Kim B. Effect of phenyl-isocyanate functionalized graphene oxide on the crystalline phases, mechanical and piezoelectric properties of electrospun PVDF nanofibers. Ceramics International. 2021;47:11010–21.

52. Jiang J, Tu S, Fu R, Li J, Hu F, Yan B, et al. Flexible Piezoelectric Pressure Tactile Sensor Based on Electrospun BaTiO3/Poly(vinylidene fluoride) Nanocomposite Membrane. ACS Appl Mater Interfaces. 2020;12:33989–98.

53. Yu L, Cebe P. Crystal polymorphism in electrospun composite nanofibers of poly(vinylidene fluoride) with nanoclay. Polymer. 2009;50:2133–41.

54. Khalifa M, Mahendran A, Anandhan S. Probing the synergism of halloysite nanotubes and electrospinning on crystallinity, polymorphism and piezoelectric performance of poly(vinylidene fluoride). RSC Adv. 2016;6:114052–60.

Table 1 Values of Bragg's angle 2θ, full width at half maximum FWHM β, intensity I, crystallite size L, interplanar distance (d), interchain separation (R), and crystalline of the diffraction peaks of composite films.

Sample	2θ	β/°	Intensity	L/nm	d/nm	R	%
Ni MOF	17.6	0.34	10732.44	24.06	0.5	0.63	
	18.7	0.42	18375.84	19.35	0.47	0.59	
	20.05	0.32	4068.33	25.34	0.44	0.55	
	22.03	0.25	2829.38	32.53	0.4	0.5	
	25.26	0.29	1540.96	28.12	0.35	0.44	
	26.53	0.17	1301.53	47.51	0.34	0.42	
	27.18	0.23	3277.67	36.11	0.33	0.41	
	28.65	0.35	3300.77	23.45	0.31	0.39	
	33.48	1.51	419.25	5.55	0.27	0.33	
	35.66	0.22	3055.04	38.31	0.25	0.31	
	28.65	0.35	3300.77	23.45	0.31	0.39	
	33.48	1.51	419.25	5.55	0.27	0.33	
	35.66	0.22	3055.04	38.31	0.25	0.31	
PVDF	19.25	1.59	12581.47	0	5.56	6.95	44
	35.12	1.93	350.88	0.02	4.58	5.73	
	40.44	4.01	1035.21	0.01	2.2	2.75	

PVDF/Ni MOF 4%	19.37	2.15	5592.97	3.79	0.46	0.57	38
	29.14	0.23	540.39	35.44	0.31	0.38	
	40.13	3.6	579.23	2.37	0.22	0.28	
PVDF/Ni MOF 8%	18.26	3.79	5383.781	2.15	0.49	0.61	32
	19.22	0.99	14821.75	8.19	0.46	0.58	
	34.61	2.7	1132.725	3.12	0.26	0.32	
	40.35	6.32	1943.502	1.35	0.22	0.28	
PVDF/Ni MOF 12%	18.45	3.71	3653.406	2.2	0.48	0.6	31
	19.15	1.05	10351.43	7.73	0.46	0.58	
	21.72	0.52	2774.004	15.77	0.41	0.51	
	34.72	2.66	757.439	3.17	0.26	0.32	
	40.27	4.81	1360.522	1.78	0.22	0.28	

Table 2 The DSC of all sample onset melting temperature $T_{m(O)}$, end melting temperature $T_{m(E)}$, peak melting temperature T_m, melting enthalpy ΔH_m, and mass fraction crystallinity X_c.

Sample Name	$T_{m(O)}$/°C	$T_{m(E)}$/°C	T_m/°C	ΔH_m (J/g)	X_c(%)
PVDF	120.12	162.94	144.94	49.2	46.99
PVDF/ Ni MOF 4%	122.82	162.11	146.33	46.8	44.70
PVDF/ Ni MOF 8%	122.11	168.33	147.62	44.4	42.41
PVDF/ Ni MOF 12%	126.44	162.63	145.94	43.8	41.83

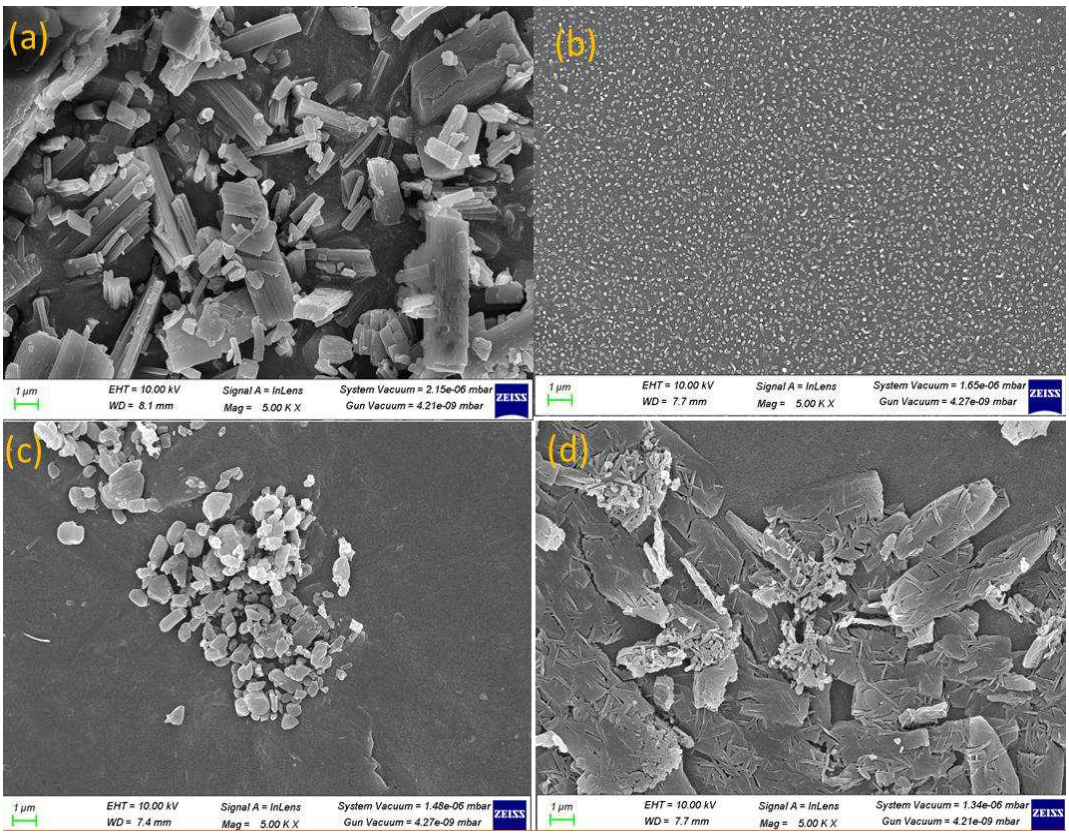


Fig. 1 SEM image for: (a) Ni MOF (b) PVDF/Ni MOF 4% (c)PVDF/Ni MOF 8%(d)

PVDF/Ni MOF 12%

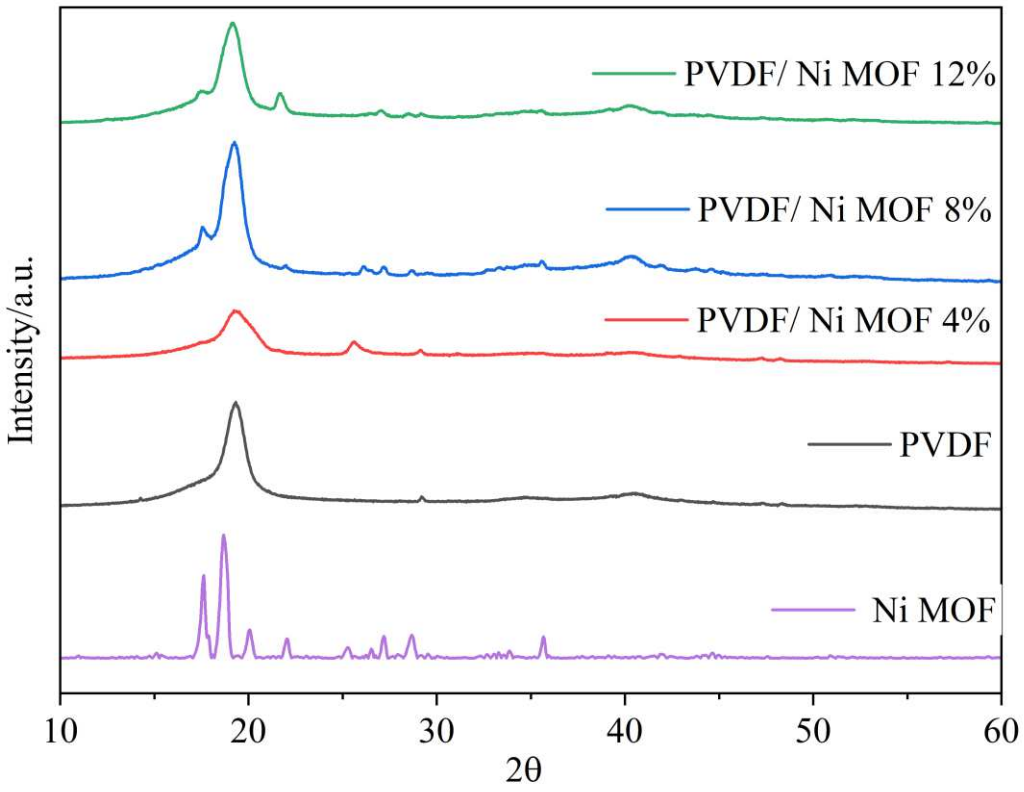


Fig. 2 X-ray diffraction pattern of polyvinylidene flouride (PVDF) and PVDF composites.

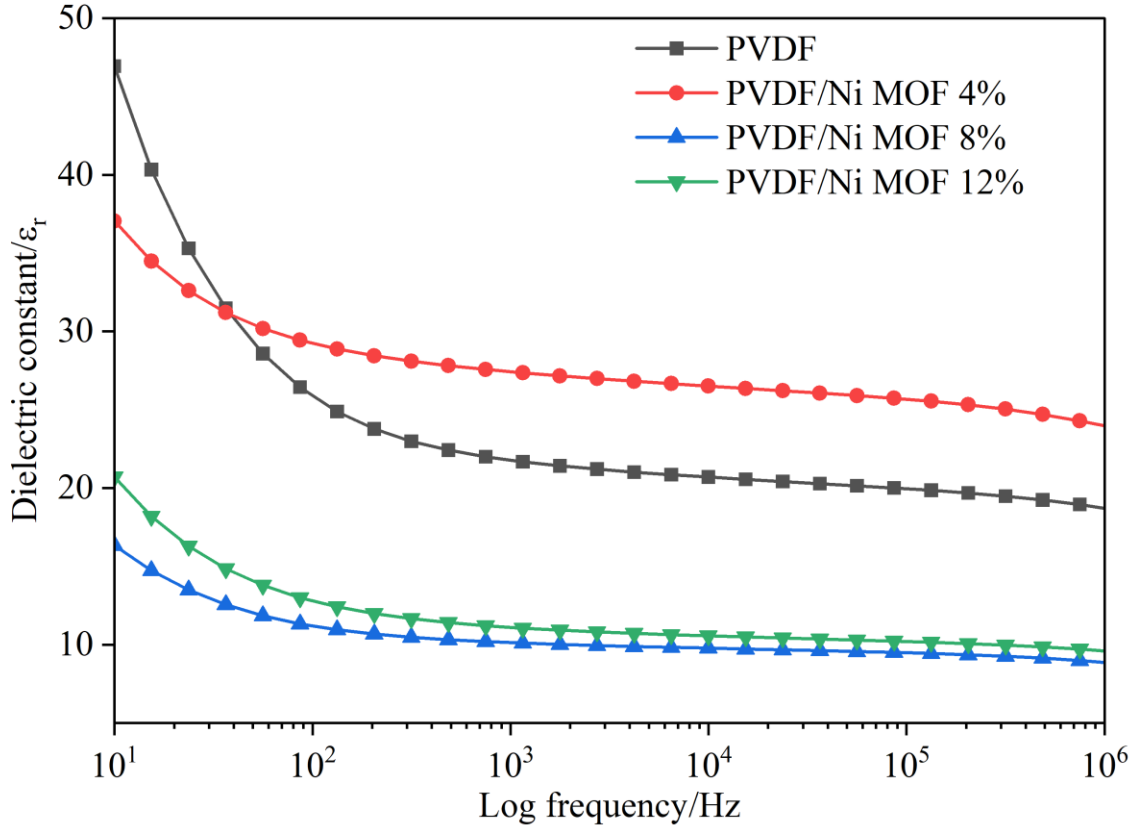


Fig. 3 Frequency dependent dielectric constant of nanocomposites at room temperature

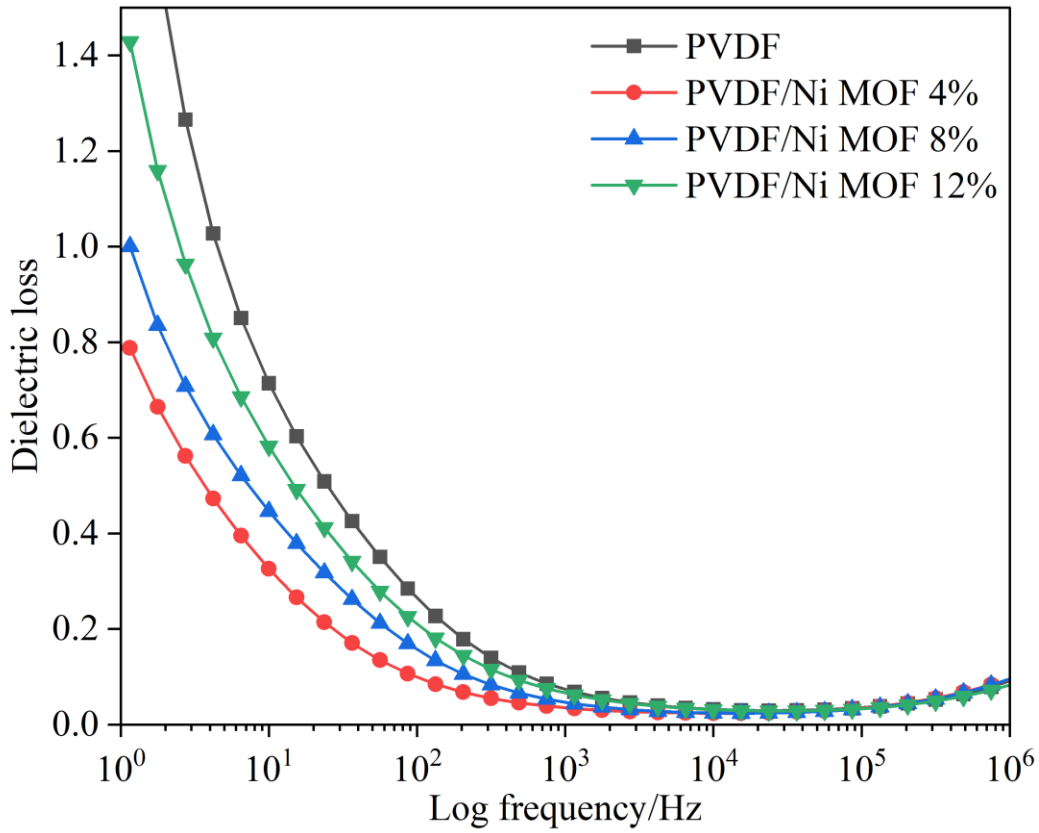


Fig. 4 Frequency dependent dielectric loss of nanocomposites at room temperature

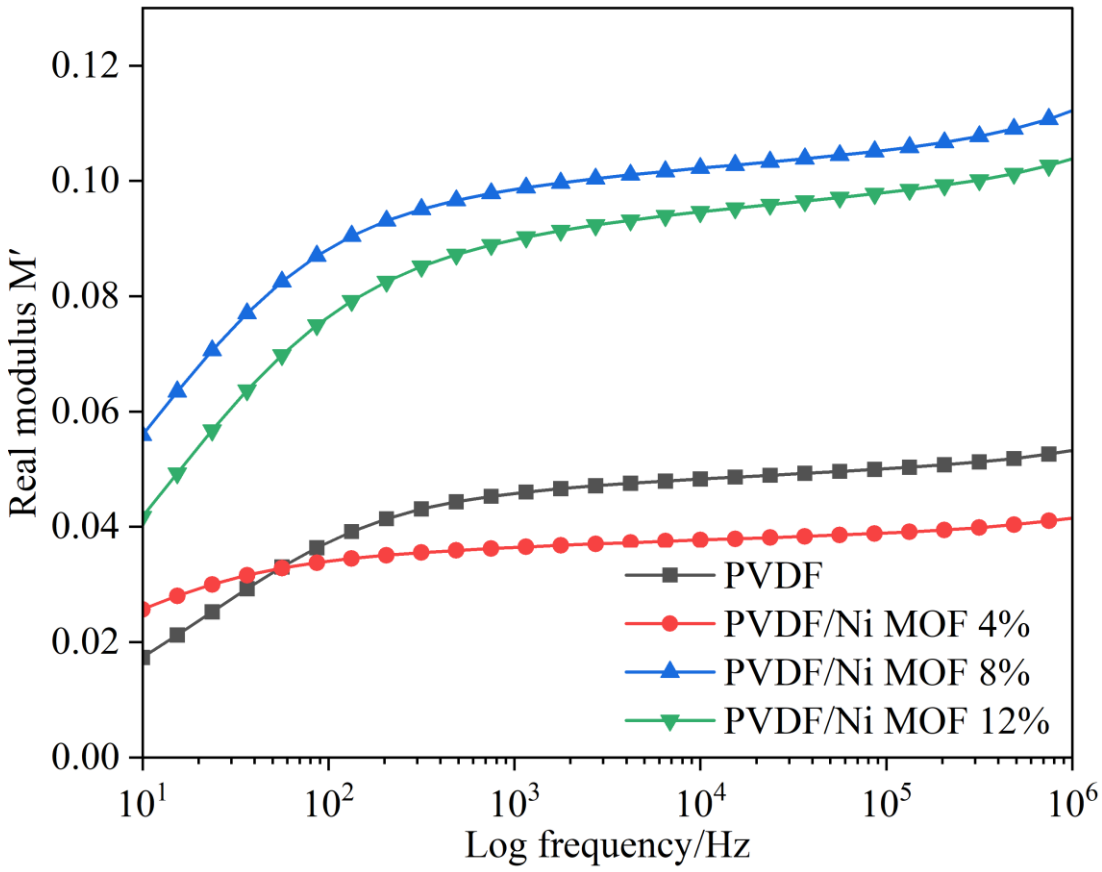


Fig. 5 Frequency dependent Real modulus M' of nanocomposites at room temperature

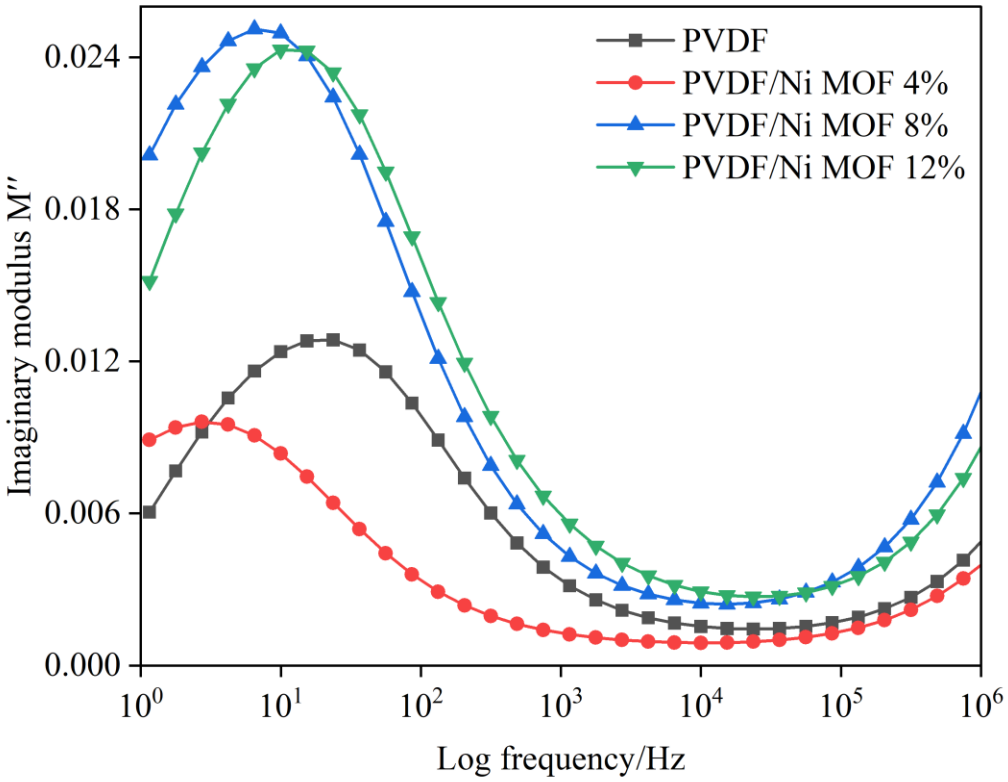


Fig. 6 Frequency dependent Imaginary modulus M'' of nanocomposites at room temperature

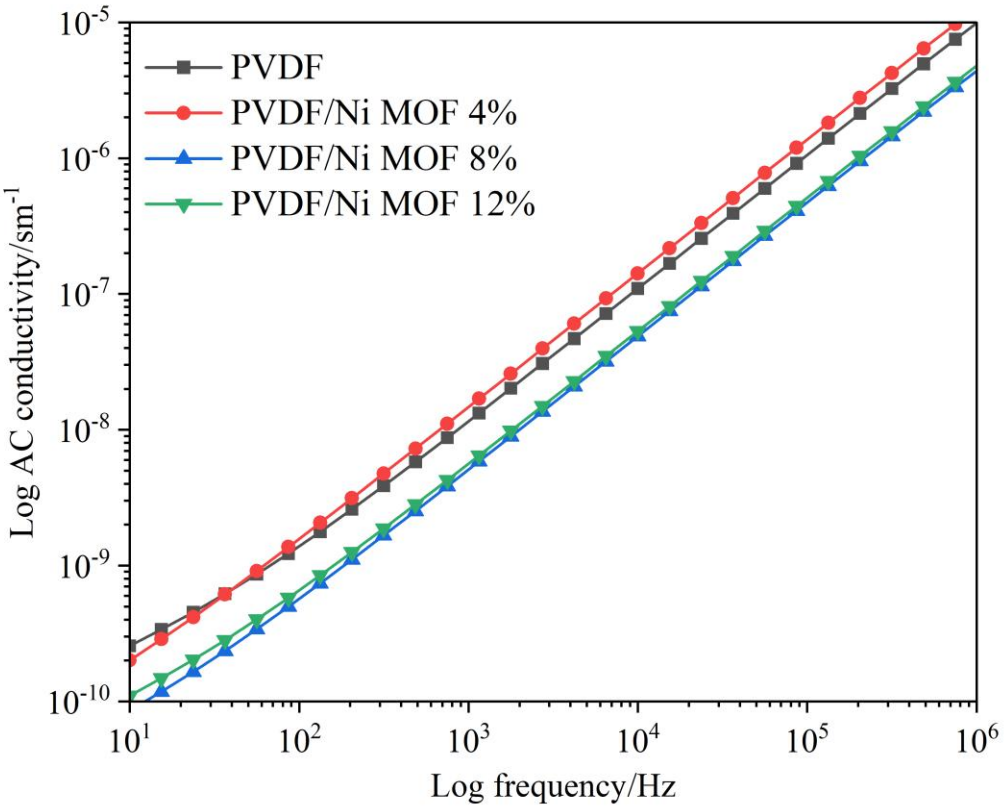


Fig. 7 Frequency dependent AC conductivity of nanocomposites at room temperature

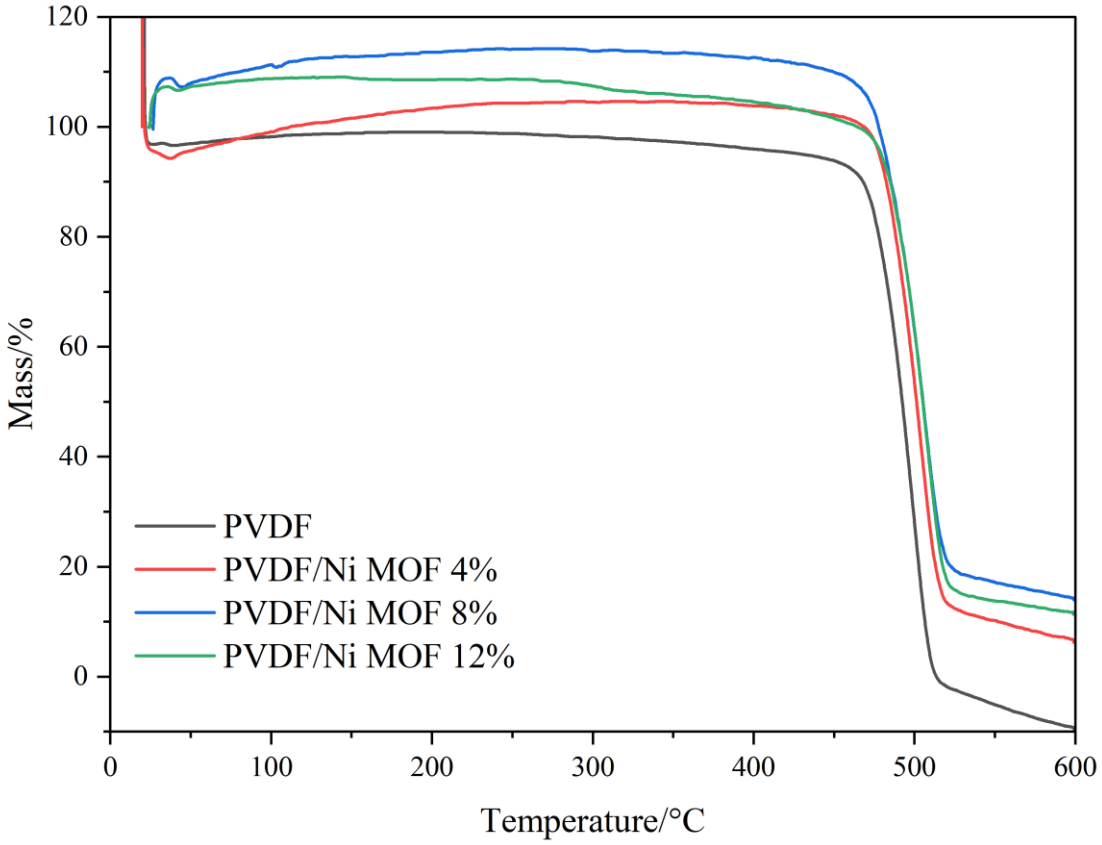


Fig. 8 Thermogravimetric analysis (TGA) curves of polyvinylidene flouride (PVDF) and composites.

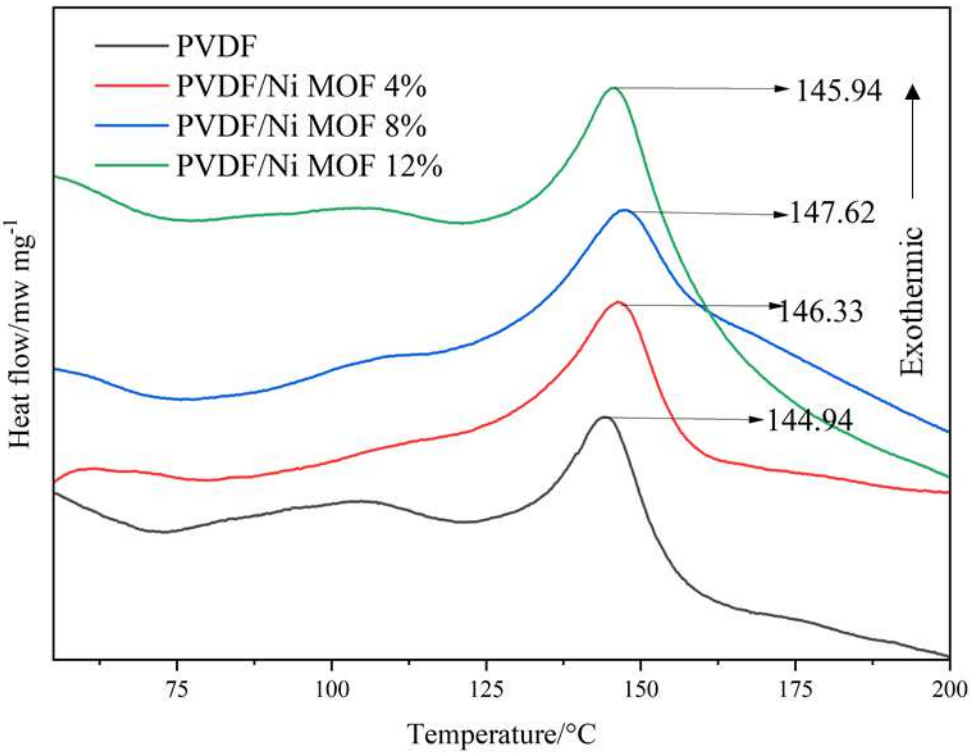


Fig. 9 The DSC analysis of polyvinylidene flouride (PVDF) and composites.